November 2015

Validation of Argon from Underground Sources for Use in the DarkSide-50 Detector

Thomas R. Alexander
University of Massachusetts Amherst

VALIDATION OF ARGON FROM UNDERGROUND SOURCES FOR USE IN THE DARKSIDE-50 DETECTOR

A Thesis Presented

by

THOMAS RYAN ALEXANDER

Submitted to the Graduate School of the
University of Massachusetts Amherst in partial fulfillment
of the requirements for the degree of

MASTER OF SCIENCE

September 2015

Physics

VALIDATION OF ARGON FROM UNDERGROUND SOURCES FOR USE IN THE DARKSIDE-50 DETECTOR

A Thesis Presented

by

THOMAS RYAN ALEXANDER

Approved as to style and content by:

A. Pocar, Chair

D. Kawall, Member

Rory Miskimen, Department Chair
Physics

DEDICATION

To dark matter! You sneaky, sneaky rascal!

ACKNOWLEDGMENTS

I am ever grateful for the wealth of helpful souls who made this project a reality. I wish to thank Andrea Pocar, my advisor and committee chair, for his insight on not only this work, but all of my research for the past three years. I would also like to thank David Kawall for being on my committee, examining my work, and offering an outside perspective that made me challenge myself to grow beyond the small bubble of research. Jane Knapp and Mary Ann Ryan each deserve a medal for their ancillary support throughout my time at UMass, as well.

A huge thank you to the staff at Fermilab that welcomed and mentored me through the final year of my graduate study. Dr. Stephen Pordes, Dr. Henning Back, Dr. W. Hugh Lippincott, and Dr. Yann Guardincerri each offered their brilliance to me as guidance, and each played an integral role in my successes. The Proton Assembly Building (PAB) is also host to the most friendly and helpful technical staff a boy could hope for. A big thank you to Bob Barger, Ron Davis, Kelly Hardin, James Humbert, Walter Jaskierny, Bill Miner, and Mark Ruschmann for assisting me and teaching me to fabricate and assemble with precision.

I would have had nothing if not for the prior work of the SCENE collaboration, whose detector I repurposed. It is to all of the collaborators, with their interest to see the hardware maintained for further science, that I thank. It is with the SCENE collaboration that I had my first up close and personal experience with an LAr-TPC, which ignited my enthusiasm for test-stand particle physics. I am also thankful to Charles Cao, the graduate student previously responsible for SCENE, for fielding my many questions during my reassembly.

Many of my fellow classmates deserve recognition for their support to me in this project. While at Fermilab, I often came home late and tired to Gary Forster and Manbir Kaur, who always kept some food on the stove and a song in my heart. I would like to thank Alissa Monte, Kirsten Randle, and the BS-DX group at UMass for their input. I cannot forget to thank Tyler Kutz and Alex Lombardi for their companionship and insight on our many late night study sessions.

The Princeton DarkSide group came to my rescue not once, but twice: evaporating fresh TPB onto the windows of SCENE and providing the hardware necessary for data acquisition. Thank you.

ABSTRACT

VALIDATION OF ARGON FROM UNDERGROUND SOURCES FOR USE IN THE DARKSIDE-50 DETECTOR

SEPTEMBER 2015

THOMAS RYAN ALEXANDER

B.A., AUGUSTANA COLLEGE

M.S., UNIVERSITY OF MASSACHUSETTS AMHERST

Directed by: Professor A. Pocar

Liquid argon is an attractive target for dark matter searches due to its low cost and exemplary event discrimination. However, atmospherically derived argon contains the beta-emitter ^{39}Ar which confounds the growth of dual-phase time projection chamber (TPC) style detectors to the ton-scale. The DarkSide Collaboration seeks to bypass this limitation by extracting argon from deep underground, from a location known to contain significantly less ^{39}Ar than atmospherically derived argon. This thesis will summarize the efforts taken to produce the first batch of underground argon, focusing on the first operation of the underground argon in a dual-phase TPC to validate the purity of the product, performed at Fermilab using the SCENE cryostat.

TABLE OF CONTENTS

LIST OF TABLES

Table **Page**

LIST OF FIGURES

Figure **Page**

CHAPTER 1

DARK MATTER DOESN'T WANT TO BE FOUND

Since the 1930s, the case for "Dark Matter" has grown from a curiosity seen far away, to one of physic's most popular puzzles, even acting as a muse for popular culture at large. From brewers and baristas to science fiction, dark matter has made itself known.

More than a buzz word for brews or a hero's deus ex machina, understanding dark matter is one of the most important questions before the scientific community today. Observational evidence of distant clusters and galaxies places 85.6% of the universe's matter as "dark," meaning that it does not interact electromagnetically. Understanding what makes dark matter tick will mean better understanding the conditions of our early universe, and give means to extend the Standard Model, which in turn would allow us new avenues of inquiry.

In 1933 Fritz Zwicky[1] brought forth the idea to account for "missing" mass needed to explain the orbital velocities of galaxies in clusters. Since then, evidences and theories have come forth, furthering the theory and directing the scientific community to new avenues with acronyms like MACHOs and WIMPs. Despite evading laboratory observation, evidence exists when looking at galactic rotation velocities, through gravitational lensing, and even the cosmic microwave background.

In the 1970s, Vera Rubin[2] obtained the first strong evidence for dark matter's existence in the form of galactic rotation in spiral galaxies, where the velocity can be measured by measuring red and blue shifts from the different arms. Rubin's findings showed a discrepancy between the luminous matter in a galaxy and the speed at

which it rotated: despite increasing radius from the center, the galactic rotational speed measured levels off quite quickly and remains inconsistently high. Figure 1.1 gives one example of this, showing the galactic rotational speed of NGC 2974 as a function of radius. Without dark matter, the rotational speed should fall off.

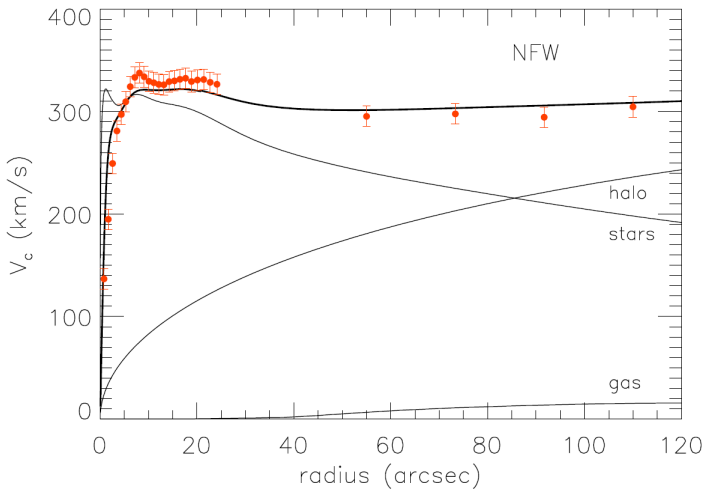

Figure 1.1: Reproduced from[3]. The rotation curve of NGC 2974.

As of 2015, two types of dark matter candidate are being funded for next-generation detectors. The more popular is the WIMP: The Weakly Interacting Massive Particle. WIMPs are a dark matter candidate that are thermal relics of the Big Bang. WIMPs are thought to exist due to decoupling from thermal equilibrium of the hot, dense plasma of the early universe. The WIMP is a candidate with an expected mass around 100 GeV, with most current WIMP searches reporting upper limits on detection cross-sections for masses between 10 GeV and 1 TeV. This corresponds nicely with the weak scale, often coined as the WIMP miracle.

The WIMP is also favored for it's ability to fit into and help confirm many popular extensions to the Standard Model, such as super symmetry or extraspatial dimensions. To the point of this publication, measurements searching to extend the Stan-

dard Model have come up wanting, increasing the fervor of those seeking to detect extensions.

1.1 Methods of Detection

Despite decades of effort and improving detector technology, laboratory detection has yet to be achieved. Combined with astrophysical probing, which gave us our first indications of dark matter's presence, there exist three possible non-gravitational interactions with WIMPs and standard model particles: Annihilation, Production, and Scattering. Together, these four methods of inquiry make of the "Four Pillars" of dark matter detection.

Annihilation of two WIMPs (χ) resulting in a pair of standard model particles

$\chi + \chi \rightarrow SM + SM$

can occur in regions of space with sufficiently large WIMP densities. In cases where the pair-annihilation process products are photons, neutrinos, or cosmic rays, detection is possible through the use of gamma-ray telescopes and cosmic ray detectors. Large celestial bodies like the Sun can capture high densities of dark matter. Experiments such as the Antarctic ice-based neutrino detector ICECUBE look to the Sun as a point source for high energy neutrinos.[4].

Colliders such as the LHC in Geneva, Switzerland look for evidence of dark matter from production pathways.

$SM + SM \rightarrow \chi + \chi + (SM)$

The (SM) denotes one or many standard model particles. While the χ cannot be seen directly in these searches due to very small cross-sections, by conservation of momentum, evidence of dark matter creation could be seen in missing momentum when summing the momentum of an event. While WIMPs could possibly be produced by the simpler process

$SM + SM \rightarrow \chi + \chi + (SM)$

they would be undetectable.

WIMPs can also, by definition, interact weakly with standard model particles. This allows a means to detect dark matter directly. Popular targets for this type of detector include cryogenic noble liquids (Argon, Xenon, Neon, and Helium), crystals (like Sodium Iodide, Germanium, and Solid Xenon), and superheated bubble chambers. In noble liquid detectors, the primary means of detection is through low energy ($\leq$ 100 keV) elastic neutron scattering resulting in observable scintillation. In crystal-based detectors, WIMP scattering results in detectable phonons in the crystal structure.

1.2 DarkSide

The DarkSide Program exists to use liquid argon based dual-phase TPC technology to search for WIMP candidates. The program focuses on background reduction as it's primary motivation. The current detector of the program, the DarkSide-50kg detector, is housed at Labratori Nazionali del Gran Sasso (LNGS) near Assergi, Italy. LNGS is an underground laboratory, employing the above mountain to act as a 3600 meter water equivalent shield. The detector itself is built with further shielding and veto capability. The LArTPC is housed inside a 4m spherical vessel containing an active liquid scintillator neutron and gamma ray veto, which is in turn housed inside a 11 meter diameter by 10 meter high cylindrical water Cherenkov veto system. The DarkSide-50 detector is expected to be able to reach a sensitivity of 10^{-45} cm^2 WIMP cross section at a WIMP mass of 100 GeV/c^2, assuming a 0.1 ton-year exposure over a three year campaign.

For direct detection experiments, background reduction is one of the most important tasks. Along with being built underground, The DarkSide-50 detector reduces its own radioactive backgrounds in multiple ways. A radon suppressed cleanroom was built directly over the vessel the detector sits in, making it possible the assemble the

detector and insert it into the aforementioned vetos without exposing the detector to natural levels of radon, which in turn minimizes the concern of ^{210}Pb plating the detector surfaces, which results in a ^{210}Po alpha background. The crown jewel of

Figure 1.2: Reproduced from[5]. The DarkSide-50 TPC.

the DarkSide experiment is the use of Argon from underground sources. Typically, argon is collected and purified from atmospheric sources. The isotope ^{39}Ar is typically present at a concentration of $8.0 * 10^{-16}$ with respect to ^{40}Ar. In LArTPCs, this results in a background with a typical rate of 1 Bq/kg. While LArTPCs are plenty capable of rejecting the ^{39}Ar background (electron events have a rejection inefficiency rate of 10^{-8}) this background becomes a burden on the data acquisition system when scaled up to ton-sized detectors, and would interfere cause a pileup with otherwise good events, rendering them unusable. The isotope ^{39}Ar is created by cosmic ray neutron interactions with ^{40}Ar. By collecting argon from underground gas wells, the DarkSide Experiment reduces this radioactive background. As of March 2015, the

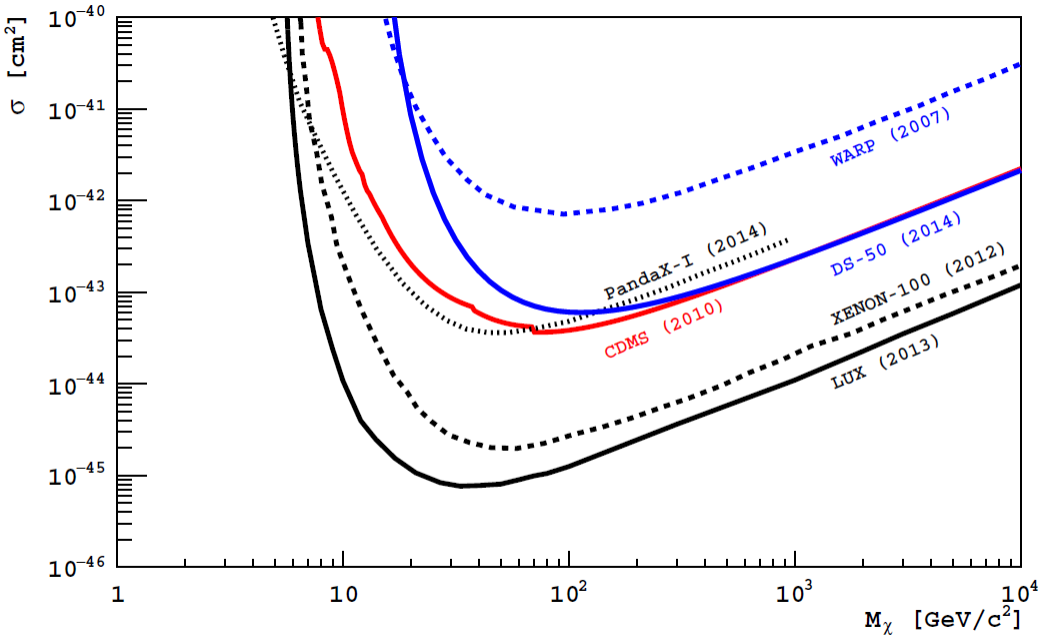

Figure 1.3: Reproduced from[5]. The first results from DarkSide-50. While DarkSide-50 will not be able to make a leading measurement in the search for dark matter, the planned 3 year underground argon run will improve upon current results significantly.

DarkSide-50 detector has run only with argon derived from atmospheric sources. The first results from this detector have been published, giving insight to where the dark matter community stands in it's efforts. Fig. 1.3 shows the current state of the spin-independent dark matter search. In blue, we have the latest search results from the DarkSide collaboration, as well as the WARP measurement. In red, CDMS's 2010 result is given. Finally, in black are the results of the Xenon-TPC, from Xenon-100 and LUX collaborations. Xenon based dark matter detectors are currently producing the leading limits on dark matter detection, thanks in large part to quality technology, but also due to a longer development lifetime. The DarkSide-50 detector, which will run a proposed 3 year data taking campaign, is a prototype for future argon based dark matter searches using underground argon.

CHAPTER 2

A NOBLE EFFORT

One technology that has received extensive amounts of attention in the dark matter community is use of liquid noble elements.[6] Argon, xenon, and other noble gases are an attractive candidate for a dark matter target for multiple reasons. Specifically considering liquid argon, the technology is highly purifiable: thanks to being mostly inert, impurities can be dealt with without concern of the argon interacting. Argon's scintillation is a product of excimer relaxation, causing the argon to be invisible to the scintillation produced. Argon produces multiple signals (Both a scintillation and ionization signal) that can be used to identify and powerfully discriminate against non-WIMP like interactions. Also attractive, liquid noble gas detectors are scalable, which is favorable to the iterative process employed by the community. Also important, and often taken for granted, the target will not decay with use like crystal detectors will, giving reliability for multiple year campaigns.

While the limit leading technology is currently liquid Xenon, liquid argon technology is catching up quickly and it is the DarkSide collaboration's intention to demonstrate the viability of liquid argon as a next-generation ton-scale target. In this chapter we will take a closer look at how liquid argon is used to detect a signal, and the hurdles the technology faces in expanding to a next-generation scale.

2.1 The Liquid Argon Dual Phase Time Projection Chamber

The type of detector used in many liquid argon experiments is referred to as a Time Projection Chamber.[7] For the purposes of dark matter detection, the ability

to track events moving throughout the detector is less interesting than the raw signals themselves. When a scattering event occurs with either the electron or the nucleus of the target atom, scintillation occurs via the aforementioned pathways. This signal is known as S1.

Along with the scintillation, the target is often ionized, creating free electrons. A negative voltage is applied to the bottom of the detector, grounded at a conducting grid near the top of the detector. Rings surrounding the detector volume graduate up from the cathode to the grid, creating a uniform electric field pointing towards the cathode. The electrons are accelerated towards the wire plane. The top of the detector is held at a high positive potential, relative to the grounded wire plane, creating a large, positive potential gradient that is used to extract the electrons from the liquid, causing a series of collisions between the accelerating electrons and the gaseous argon above the liquid. This creates a second pulse, proportional to the number of electrons extracted.

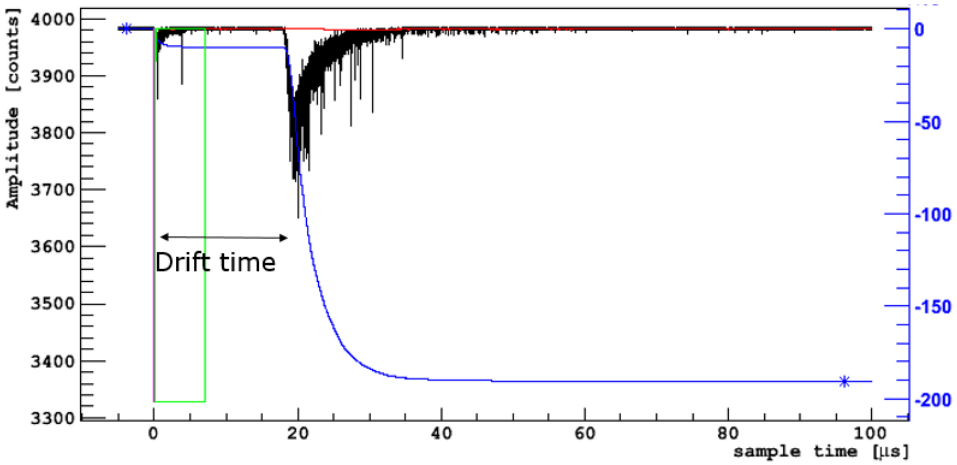

Figure 2.1: Example of an event with both S1 and S2 signals, from this campaign. Black scale is ADC bins, blue is the integral in units of photoelectrons. The left pulse is S1, while the right signal is S2. The time between these two pulses is known as the drift time. In the case of this event, which was taken in a drift field of 200 V/cm, we can calculate that this event took place in the center of the top half of the detector. The maximum drift time at this field strength is 80 μs.

The timing between these two pulses is known as the drift time, and can be used to track the position of the event along the axis of the electric field. The drift speed of electrons in liquid argon has been measured for multiple drift field strengths, so position can be calculated with confidence. In detectors with large arrays of photosensors on the top and bottom, the position of an event can be reconstructed in 3 dimensions. In high energy events where the incident particle scatters multiple times over a long path, this combination of pulse and ionization tracking allows for event reconstruction, giving the TPC its name.

2.2 The Effect of Impurities

In theory, most of the light emitted during scintillations should be capturable by photosensors, assuming reflective foil is used to gather light not directly aimed at the photosensors. Similarly, most of the electrons ionized should be able to drift freely to the top of the detector, with only ionized argon atoms accepting the free electrons. In practice, however, there are several hurdles that limit signal quality.

Both the scintillation signal and the ionization signal are known to be adversely affected by small concentrations of impurities. The impurities of most common concern are those found in air, the source from which commercially available argon is typically purified from. The ionization signal can be adversely affected by part per hundred trillion levels of oxygen and water, and nitrogen must be controlled to part per million levels to prevent scintillation quenching and absorption.[8] Scintillation quenching is observed when an impurity disassociates argon excimers from an event, and reducing the amount of light that occurs late in the event. Scintillation absorption refers to the loss of light due to impurities opaque to the 128 nm scintillation interacting with the emitted light from an event. A concern to the DarkSide Collaboration is methane, a product found at levels of 5700 ppm in the initial gas from the CO2 well in Cortez, CO. While methane will not effect the ability to drift electrons

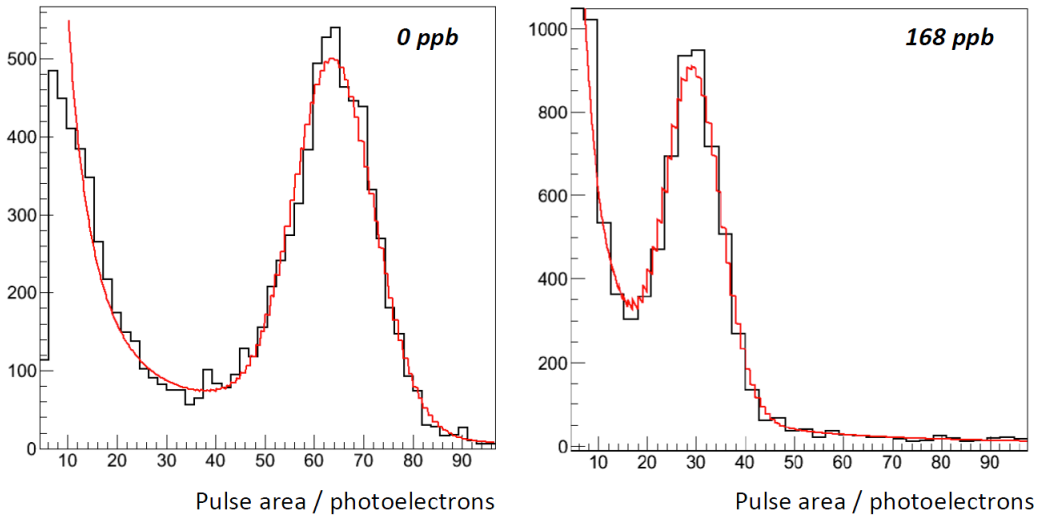

Figure 2.2: Reproduced from Ref. [9] Comparison of pulse integrals for liquid argon with 0 ppb methane and with 168 ppb methane.

for an ionization based signal, methane concentrations larger than 10 parts per billion have been shown to greatly reduce the amount of light collected from scintillation. This amount of methane is well below the sensitivity of the UGA in place to analyze the gas during purification. Methane primarily reduces the observed scintillation by absorption, though at concentrations greater than 40 parts per billion quenching is observed, as well.

2.3 Argon Scintillation

Liquid argon is an incredible asset in the search for dark matter. Scattering off of argon atoms yields a scintillation from two different processes. Scintillation can occur via direct excitation:

$$Ar^* + Ar \rightarrow Ar_2^* \tag{2.1}$$

$$Ar_2^* \rightarrow 2Ar + h\nu \tag{2.2}$$

or via ionization:

$$Ar^+ + Ar \rightarrow Ar_2^+ \tag{2.3}$$

$$Ar_2^+ + e^- \rightarrow Ar^{**} + Ar \tag{2.4}$$

$$Ar^{**} \rightarrow Ar^* + heat \tag{2.5}$$

$$Ar^* + Ar \rightarrow Ar_2^* \tag{2.6}$$

$$Ar_2^* \rightarrow 2Ar + h\nu \tag{2.7}$$

Thanks to a large stokes shift, this process can produce scintillation that is not immediately reabsorbed; the dimer would have to be in a vibrational excited state almost 1 eV above the ground state to reabsorb the light.

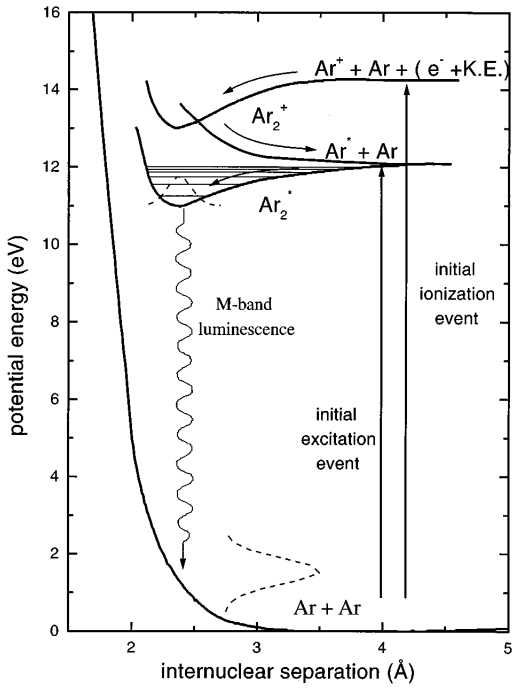

Figure 2.3: Reproduced from Ref.[10] Diagramatic description of the argon scintillation pathway.

Liquid argon also has a fantastic ability to discriminate between electron recoils and nuclear recoils, based on the signal vs time's shape. Dictated by argon excimer density, either a singlet or a triplet state excitation will occur. The singlet state is very short lived (6 ns) compared to the triplet state (1.5μs.) Nuclear recoils will result

in mostly singlet state scintillation, placing most of the event light within the first 90 ns of the event, whereas electron recoil events will have a much higher density of triplet state scintillation, and most of the light will not be in a window of the first 90 ns of an event. The proportion of light in this window to the total light collected from the event is known as the pulse shape discrimination parameter F90. Electron recoil events typically have a F90 of 0.3, neutron recoils 0.7. This a very clear, powerful discrimination technique. A WIMP event in the detector would be a nuclear-recoil event.

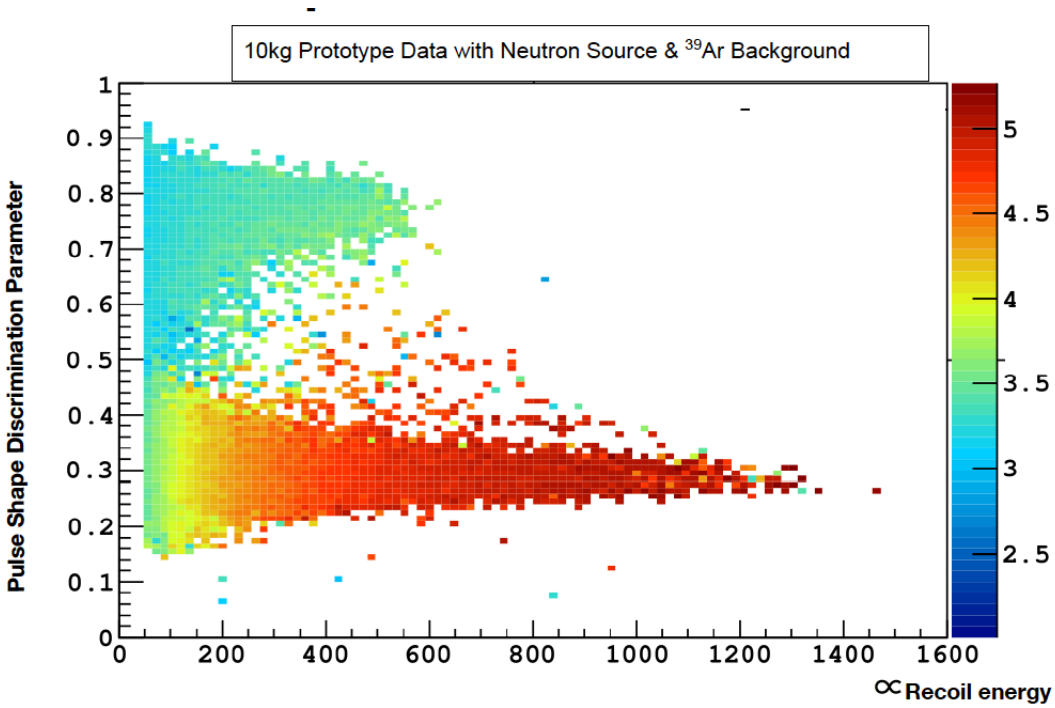

Figure 2.4: Reproduced from Ref.[11] A visual of the pulse shape discrimination parameter vs the S1 signal. Nuclear recoils are the upper peak, while electron recoils (in this case from ^{39}Ar are the lower peak.

The ratio of the scintillation and the ionization signal can also be used to discriminate between nuclear and electron recoils. The lower density of electron-ion pairs results in less recombination, leading to a larger S2 signal compared to nuclear recoils of the same S1 energy.

2.4 Underground Argon

In dark matter searches using liquid argon, a primary background is the radioactive isotope ^{39}Ar. ^{39}Ar is a beta emitter with an endpoint energy of 565 keV. Because it will cause electron recoils in liquid argon, it is easily discriminated against using the F90 parameter. However, as detector size increases with each generation, the number of events starts to become a burden on the data acquisition system. If the detector is a dual phase TPC, the long event times necessary to observe slow drifting electrons increases the amount of time the data acquisition has to spend detecting ^{39}Ar events, effectively dead time. With a rate of 1 Bq/kg of liquid argon, ^{39}Ar events can also interrupt events, possibly removing WIMP-like events from being properly scrutinized.

Large single phase detectors[12] are much less sensitive to this issue, since they do not drift electrons. Neutrino detectors typically look at much higher energy events than dark matter detectors and will have a higher threshold for event data collection than a ^{39}Ar event could trigger.

For the DarkSide Experiment, the question then is how to remove this background. Traditionally gathered argon contains ^{39}Ar. ^{39}Ar is a beta emitter with an endpoint energy of 565 keV. The lifetime of this isotope is 269 years, making it impossible to simply "wait it out." The only feasible way to reduce the presence of ^{39}Ar would be through isotopic separation via centrifuge or distillation. This has previously been considered prohibitively expensive, however the effectiveness of this option is currently being investigated for the future of the DarkSide program.

Most of the earth's atmospheric argon was produced by electron capture of long-lived ^{40} via the process

$$^{40}K + e^{-} \rightarrow ^{40}\ Ar + \nu \tag{2.8}$$

using potassium found naturally in the earth. ^{39}Ar is created in the atmosphere via interactions with cosmic rays and ^{40}Ar. Below the Earth's surface, ^{39}Ar can be created via neutron capture by ^{39}K or calcium emission by calcium. Observation has shown that the earth's crust has only slightly lower rates of ^{39}Ar, due to a sequence of nuclear reactions starting with the alpha particles from the decay of uranium or thorium and their products to produce ^{39}Ar by the (n,p) reaction on stable potassium. In the Earth's crust, this stable potassium is found at a concentration of a few percent, and uranium, thorium are found at concentrations of parts per million (ppm.) Fortunately, if you go deeper, into the mantle of the Earth, uranium and thorium are thought to be found at the part per billion level.[13]

The purpose of retrieving argon from deep underground wells is to create a product with a greatly reduced ^{39}Ar content. ^{40}K is still present underground, allowing for the creation of ^{40}Ar, however the crust of earth above the point of production greatly decreases the creation of ^{39}Ar from cosmics. While ^{39}Ar is measured to be $8.0 \pm 0.6 * 10^{-16}$ in the atmosphere, this is still a significant background in large detectors.

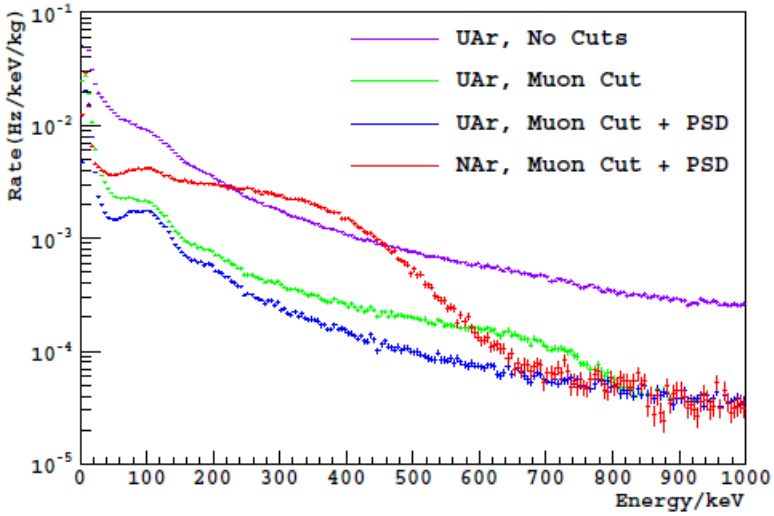

Figure 2.5: Reproduced from Ref. [14] Spectrum observed in atmospheric and underground argon runs at KIRF. ^{39}Ar is present in the atmospheric argon sample (red) but greatly diminished in the underground argon cell (blue.)

This study is not the first to look at the underground argon. In 2012 members of the DarkSide Collaboration took gas collected from the Cortez, Colorado gas well to analyze how much ^{39}Ar was present in the gas well. Collected gas was condensed and observed at Kimballton Underground Research Facility (KURF.) The space used at KURF featured a 1450 m water-equivalent shield, allowing for a much more precise measurement of the ^{39}Ar than would be possible on the surface, due to background events from cosmic rays. 0.56 kg of liquid argon was observed for a period of 200 hours, giving a dataset of approximately 100 kg*hrs.

The signal was analyzed conservatively by accounting for other backgrounds, including PMTs and a ^{252}Cf source from a nearby experiment. The background from the detector itself was not measured. With the backgrounds subtracted, the remaining rate of 0.32 $\pm$ 0.23 mBq was measured. From an upper limit confidence interval of 95%,the experiment found that the underground argon had an upper limit rate of 0.65% the atmospheric rate. This emboldened the collaboration to double-down on production efforts of the Underground argon.

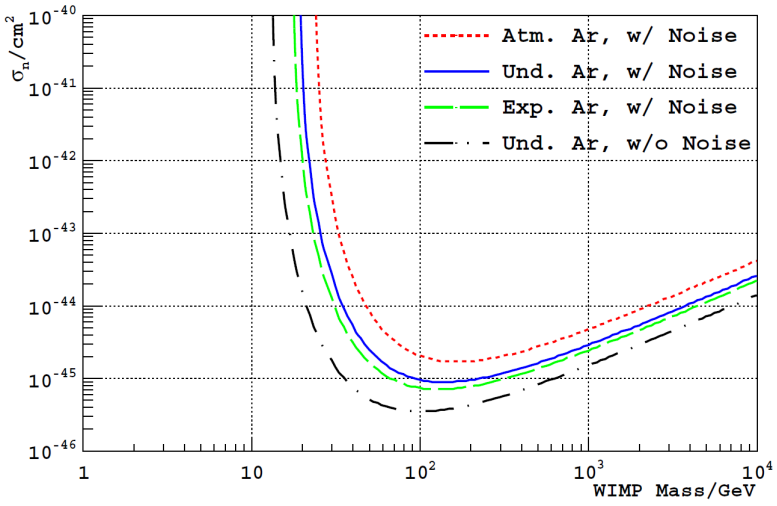

Figure 2.6: Reproduced from Ref. [14]. Comparison of the expected survey results from a 1 ton*yr search comparing atmospheric argon to the upper limit of 0.65% the atmospheric argon rate, and an expected lower rate of 0.1%.

The primary function of the underground argon is to reduce the electron-recoil background rate in the darkside, and this has wide-ranging effects. Most importantly, the reduction of this significant background will reduce the amount of deadtime experienced by the system attempting to collect these events. Another important aspect of this reduction will be an improvement to detector threshold. By reducing the major electron-recoil background rate, nuclear recoil acceptance will improve for low energied events. This results in large (50x) gains at low masses. Note that Fig. 2.6 uses only simple discrimination techniques to produce a comparison between the underground and atmospheric argon, and the sensitivity of DarkSide-50 is expected to be better than projected by the figure.

2.5 Underground Argon Processing

Processing the Underground Argon starts in Cortez, Colorado. Gas is pulled from wells at the Kinder-Morgan Doe Canyon CO2 facility.[15] By maintaining a small production plant built to accept the waste output from the CO2 processing plant, argon from deep in the mantle is collected. The carbon dioxide well is comprised of 96% carbon dioxide, 2% nitrogen, and a balance of other gases. Argon has been found to be 600 ppm in this well. The waste gas is ran through a series of two zeolite filters in a vacuum-pressure swing adsorption system. The output from this system is a mixture of helium, nitrogen, precious argon, methane, oxygen, and various hydrocarbons. Production has varied over the years, but typically the plant has produced several hundred grams of argon per day.

The collected gas is then sent in bulk to Fermi National Accelerator Laboratory in Batavia, IL where it receives further refinement.[16] The mixture is condensed at 76 K through the use of a low pressure liquid nitrogen jacket. This leave helium as a gas, which is vented off through a trap of charcoal. The charcoal trap is submerged in liquid argon, allowing the helium to be vented off and recapture the argon vapor

pressure. Argon recaptured on the charcoal is sent back to the helium seperator until it is ready for further purification. The collected liquid is vaporized and sent through

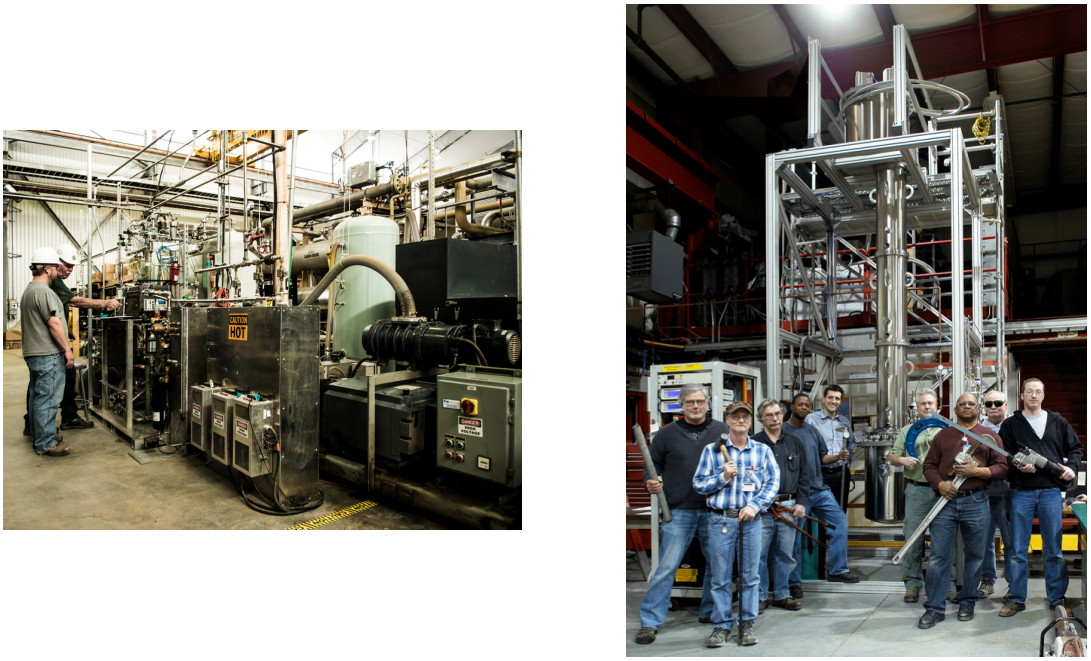

Figure 2.7: Left: The VPSA plant located at Kinder Morgan in Cortez, CO. Right: The distillation team with its team. Both images photocredit the DarkSide Collaboration.

piping cooled to 105K to freeze out a known carbon dioxide impurity, as well as any other (typically) high mass unknowns without liquefying the argon or nitrogen. The mixture then passes through a Hi-Cu oxygen getter developed by Research Catalyst, Inc. This getter removes the product from levels of $> 1\%$ to less than part-per-million levels, below the sensitivity of the in line gas monitoring residual gas analyzer. The remaining gas is almost exclusively nitrogen and argon, with trace amounts helium that was not previously vented, due to mixing in the liquid while in the helium separation phase.

A cryogenic distillation column was built at Fermilab to separate the argon and nitrogen, leaving a mostly pure product of underground argon. Analysis is done with an SRS UGA-300 residual gas analyzer, allowing us to measure nitrogen levels in

the product to a part per 10,000 level. Further analysis of the gas is done at Pacific Northwest National Lab, and has shown the distillation column is capable of removing nitrogen to the parts per million level.

While mostly pure, some contaminants both known and unknown are still in the gas at very low (ppm) levels. The final stage of the purification takes place at the DarkSide-50 detector. A heated zirconium getter is placed in line with the gas condensing system of DarkSide-50, purifying the argon one last time before being deposited into the detector. The zirconium rare-gas getting material used claims to remove water, CO2, acids, bases, organics, and refractory compounds to a limit of 1 part per billion, making it an ideal final step.

2.6 Motivation for Study

The DarkSide Experiment seeks to use argon purified from underground sources to reduce backgrounds and prepare for a next generation detector. Purification has been accomplished in-house via several effective methods of separation, leading to a product thought to be highly pure. However, the gas has not been proven to be an effective scintillator - unexpected impurities could suppress light created by the argon, rendering the target ineffective. Before shipping the purified argon from the purification plant at Fermilab, USA to the detector at LNGS, Italy, the quality and capability of the gas as a detector target must be assured. To test the viability of this gas, a small dual-phase TPC has been used to test the ability of the purified underground argon, and compare it to commercially available research grade argon from atmospheric sources.

Though a larger detector volume is being used than previous measurements on the UAr, this measurement is not able to measure the ^{39}Ar content in the product being prepared for shipment. If this measurement were performed at an underground facility, such a measurement would be possible, however this measurement is meant to

verify the gas as a scintillator and as a charge drifting medium. A radioactive source, along with a wide spectrum of cosmic rays, increase the rate of event counting and bury the relatively small ^{39}Ar background.

CHAPTER 3

APPARATUS

The SCENE detector[17][18] was originally built to be a portable dual-phase liquid argon time projection chamber capable of being transported to Notre Dames Institute for Structure and Nuclear Astrophysics. This largely influenced the outer detectors geometry and functionality.

3.1 Gas Handling

Input gas first passes through a SAES monotorr getter[19] before entering the detector. When active, the gas also flow through a rubidium trap to input a uniform ^{83m}Kr source into the detecting volume. Pressure relief valves were placed throughout the gas handling system and connected to the detector volume to insure pressure did not exceed 15 psig, to protect the photomultiplier tubes.

The detector is closed off and suspended in a cryostat that is used to create a vacuum in the region outside the detector volume. Further, the detector is wrapped in super insulation. The combination of these two factors help minimize heat transfer to the detector, reducing unwanted boiling effects.

Liquid argon is condensed by a Cryomech PT60 helium compressor[21] and into the detector volume. A heat exchanger exists to cool incoming gas with outgoing gas in a recirculation loop.

A series of three PT1000 thermoresistors are used to track the liquid level as it approaches the detector volume, while a 3 radially symmetric capacitors are used to measure the precise liquid level near the hexagonal grid. The three capacitors can be

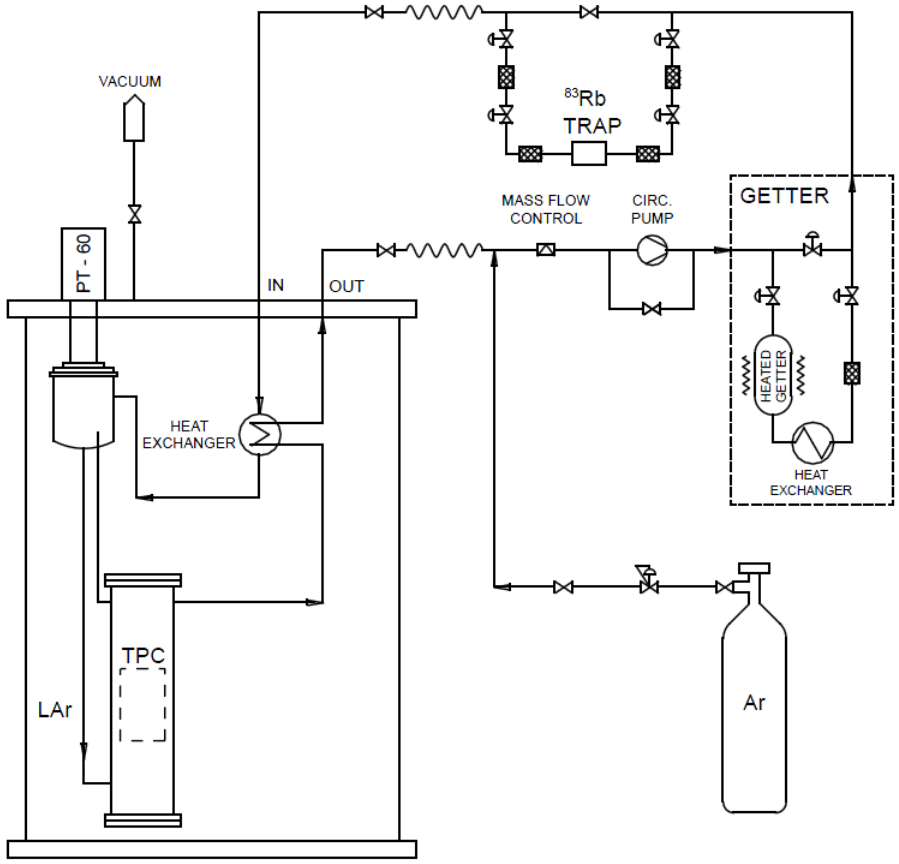

Figure 3.1: Reproduced from Ref. [20] Schematic of the SCENE detector and related gas-handling system.

used to calculate a plane and insure that the liquid level in the detector is even across the whole grid. Unfortunately, one of these sensors was damaged during reassembly and so this functionality was not in place for this test.

The gas recirculation pathway includes a ^{83m}Kr source akin to the calibration source used in DarkSide-50, and described by [22]. The radioactive source enters the detector as a gas, creating a uniformly distributed source throughout the detector volume. ^{83m}Kr is produced by the decay of ^{83}Rb (τ=124.4 days), which is absorbed on a synthetic charcoal trap as RbCl. The ^{83}Rb remains trapped on the charcoal while the ^{83m}Kr is free to pass through a small filter and into the detector. The ^{83m}Kr has

Figure 3.2: The TPC with PMTs and level and temperature montoring hardware as prepared for this campaign. As compared to previous campaigns with the SCENE Detector, a PTFE cylinder was added to the base of the detector volume to reduce the amount of argon required to fill, with the security of the Underground Argon in mind. Otherwise, the setup remains the same as previous, published campaigns.

a lifetime of $\tau = 2.64$ hours, making it possible to introduce the gas source and "remove" it with time. The ^{83m}Kr decay is a sequence of two electromagnetic decays of 32.1 keV and 9.4 keV with a mean seperation of 222 ns. Due to the length of the argon scintillation's triplet state component (1.5μs), the two decays are effectively seen as a single deposit of 41.5 keV. At the time of campaigns presented here, the source was quite cold, only offering a signal rate of 20Bq.

3.2 The TPC

The TPC was built to mimic the TPCs used by the DarkSide series of detectors. The TPC is built out of polytetrafluoroethylene (PTFE) with a 76 mm outer diameter. The active region is a 68.6 mm in diameter by 76.2 mm tall cylinder. Above the active region is a thin steel mesh grid, used to define the grounding point in the TPC. The strips of the hexagonal grid are 50 micrometers wide, with the opposing sides of each hexagon being 2 mm apart. Above the hexagonal grid is a space 7 mm in height that, during operations, contains gaseous argon. The space below the grid is filled with liquid argon.

Surrounding the active region are 12 copper rings connected with 100 MOhm resistors acting as a voltage divider. During operations, the bottom ring acts as the detectors cathode and is held at a high (kV) negative potential relative to the grounded hexagonal grid. The series of rings creates a uniform electric field within the active region to drift electrons with. Conversely, 7 mm above the hexagonal grid is a single copper ring with no local connection to the ground. It is held at a high (kV) positive potential relative to the grounded grid, creating a very strong "extraction field" to pull freed electrons out of the liquid and accelerate them to the anode.

Above the Anode and below the Cathode is a cylindrical quartz glass window, with an Indium-Tin Oxide (ITO) coating on both circular faces. The circular plane of each window facing the active detector region are further coated with a layer of

Tetraphenyl Butadine. (TPB) The ITO layer acts as a conductor, allowing the full face of the window to be held at a constant potential consistent with the anode or cathode copper ring it is held against by the PTFE structure. The TPB acts as a wavelength shifter to bring the argon scintillation to the near VUV range, where the photomultiplier tubes are most sensitive. The PMTs are insensitive to the native 128 nm scintillation from the argon. A thin 3M reflective foil[23] was placed inside the copper field rings, and layer of TPB was evaporated on to it as well as the windows, effectively creating full coverage of the wavelength shifting material.

Due to the importance of the TPB coating on the observable signal, the TPB coating was redone prior to the campaign presented here. The TPB previously on the windows had degraded from multiple campaigns, and degradation from storage. Research purity ($> 99\%$) TPB produced at Sigma Aldrich[24] was evaporated onto the windows at Princeton Univeristy to a specification of $200\mu g/cm^2$, the specification used for previous runs of the SCENE detector and from data presented in ref.[25]. Unfortunately, due to a severe shortage of the high purity TPB available, only the windows were recoated; the 3M reflector foil that enclosed the radial face of the detector volume was left as-is.

Hammamatsu R11065 PMTs[26] were trusted to collect light from the active volume. The PMTs face is pointed towards the active region and ran at a potential of -1600 Volts. While the bottom PMT is held in liquid argon, the top PMT is held in the gas phase at all times, and over several campaigns in the SCENE detector has endured several shorts, decreasing the quality of this tube. However, to maintain fidelity with previous runs, this PMT was still used.

3.3 Signal Processing

The two Hammamatsu photomultiplier tubes are held at a voltage of -1600V. The analog signal is fed into a CAEN V1720 Digitizer.[27] Because of the simplicity of

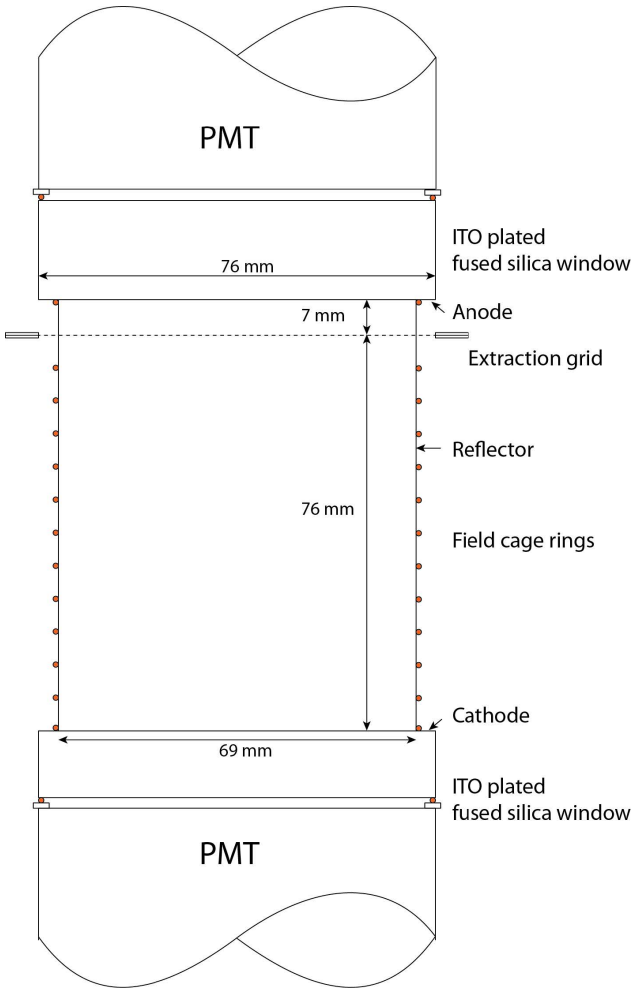

Figure 3.3: Reproduced from Ref.[20]. Diagram of the TPC geometry with measurements.

the trigger logic, the trigger was handled by the V1720 software. A threshold of -10 mV was set and a signal in both PMTs was required for the event to be recorded. A CAEN A2818 was responsible of interfacing the Digitizer to the data acquisition computer. A data acquisition package known as DAQman[28], developed for the DS-10 prototype detector, was employed to handle data collection and analysis. Because the SCENE detector uses the same digitizing boards, the same PMTs, and generally the same variables of interest, it was a natural fit for the experiment. DAQman has many useful features to both interface with the digitizer and also create coherent run and event data from the incoming waveforms.

3.4 Hardware Monitoring

Detector temperature was controlled using a LakeShore 336.[29] The Lakeshore 336 handled temperature control at the condenser using a temperature probe and heater in a brass plate connected to the PT60 refrigerator. Power to the heater block was dictated by the Lakeshore's PID capabilities. The temperatures in the liquid and gas regions of the detector, as well as the heater power output were read in from the Lakeshore and recorded to a PC using LabVIEW.[30] The LabVIEW interface also connected with a Measurement Corporation PWD-1208ls[31] ADC to measure the pressure and mass flow at the gas handling rack, as well as rudimentary liquid level measurement using PT-1000 thermistors. Finally, a capacitive liquid level measurement was taken by a Smartec UTI[32] 5 channel capacitance reader to precisely bring the liquid level above the grid. The capactive reader measured 3 small parallel plate capacitors situated radially equal and equally spaced (120 degrees to center.) The device was capable of millimeter resolution, allowing the detector to be leveled to create a uniform liquid level above the grid. Unfortunately, for this test the leads of one of the three capacitors was damaged during detector insertion. Liquid level uniformity was achieved using the remaining two capacitors and monitoring for the presence of S1 + S2 events using a Tektronics oscilloscope.

3.5 Emergency Recovery System

The underground argon used in this test was a precious resource, and recovery of the gas without contamination was a priority. Nearly 4 kg of argon was required to fill the detector, at the time this was nearly a month's worth of production at the plant in Cortez, CO, not including purification at FNAL.

The hardware monitoring system was connected to a 30 minute battery backup, "a Laptop," and was programmed to send alerts, "text messages," in case of emergency.

A simple system to recollect the underground argon was created, repurposing the helium separation system of the distillation system. This insured that even in the event of a power outage or cryocooler failure, the gas would be saved. The helium separation system was kept at a pressure of 8 psig, and a check valve was placed leaving the SCENE detector at a differential pressure of 3 psi. If the pressure rose in the detector beyond 11 psig, gas would be exhaled into the helium separator, which was held at liquid nitrogen temperatures. This insured any argon "lost" due to emergency would be recondensed for purification.

Luckily, there was no emergency, though this system was employed following the completion of the campaign, for the same purpose.

CHAPTER 4

ANALYSIS

The Atmospheric Argon run of this campaign lasted from November 14th until December 8th, and was also used for troubleshooting. The comparatively long length of this campaign allowed the argon extra time to purify, though attempts were made to remain "stable."

The Underground Argon run of this campaign took place from December 13th until December 18th (4 days.) Data collection for S1 only, with the liquid level above the face of the top PMT, occured for the first 24 hours. The recirculation rate was ramped up to 6 slpm over 4 hours, with a heat load of 30 Watts added to the bottom of the detector for bubbling. Following this, the liquid level was brought down to just above the field grid, where S2 events were observed. Rigorous recirculation (6 slpm recirculation flow, bottom heater at 90 V) occured through the next day. The recirculation rate was then brought down to 3 slpm and the bottom heater was set to output just 30V*R of power. After sufficent S1+S2 data was collected, recirculation resumed, and was paused for purified measurements of S1 parameters.

Typically, the S1 parameters would be measured with the liquid level above the face of the top PMT, however the decision was made to not adjust the liquid level again. Concerns were present of helium back-contamination from the helium separator that acted as the recovery system for the argon, so the only method to lower the liquid level was by venting to atmosphere.

The drift field was held at -200V/cm for most of S2 data collection. The drift field was lowered to -50V/cm to look at drifting over a long period of time. The extraction field was always held at +3000V/cm for all S2 data collection.

Four parameters were measured to qualify the underground argon. Two of these tests were related to the initial scintillation (S1) and other two were related to the scintillation caused by the ionized electrons (S2.)

4.1 Event Selection and Triggering

Event selection for this campaign was very straight-forward. For S1 only runs, events were required to not saturate the ADC, and were required to have an f90 prompt between $0.2 < f90 < 0.4$. While in S1 + S2 mode, the events were additionally required to have a minimum drift time of 7 microseconds, to reduce the chance of S1 and S2 overlap. Triggering was accomplished directly on the digitizer, set to require a minimum of 1 PE in both of the PMTs for the event to be collected.

4.2 Single Photoelectron Calibration

Understanding the PMT response is crucial in being able to say anything at all about the argon being used. PMT calibration was done by looking for small pulses in the tail of the events. For S1 only events, the pulses were searched for in the last 5 microseconds of the whole 20 microsecond window. By looking at the minimum amplitude of the integral of a pulse we can find the PMTs response to a single photoelectron from the photocathode. This is the smallest signal possible, and the unit that all pulses will be measured by going forward.

The pulse selection tool identifies small aberrations from the baseline as pulses, so multiple PE pulses are also collected. To account for this, the spectrum created is fit to a series of 4 Gaussian peaks, with the mean and standard deviation of the first

Gaussian being the measurement of interest. Further analysis uses this as the unit relatable to energy.

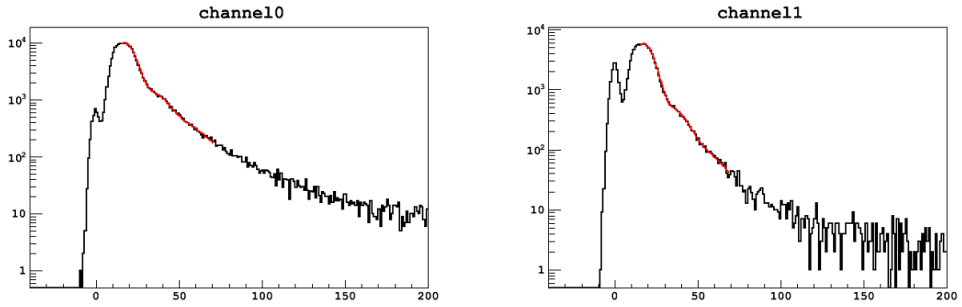

Figure 4.1: Results of the fits to an S1 only run. The mean of interest is the well defined, leftmost peak in red. Channel 0 is the bottom PMT, while Channel 1 refers to the top PMT.

4.3 Light Yield

The powerful ability of liquid argon to discriminate between recoil types is largely based on the ability collect as much of the light as possible. Because of this, the ability to measure the light yield, how much light is being collected per keV of energy deposited, is incredibly important to liquid argon TPC calibration.

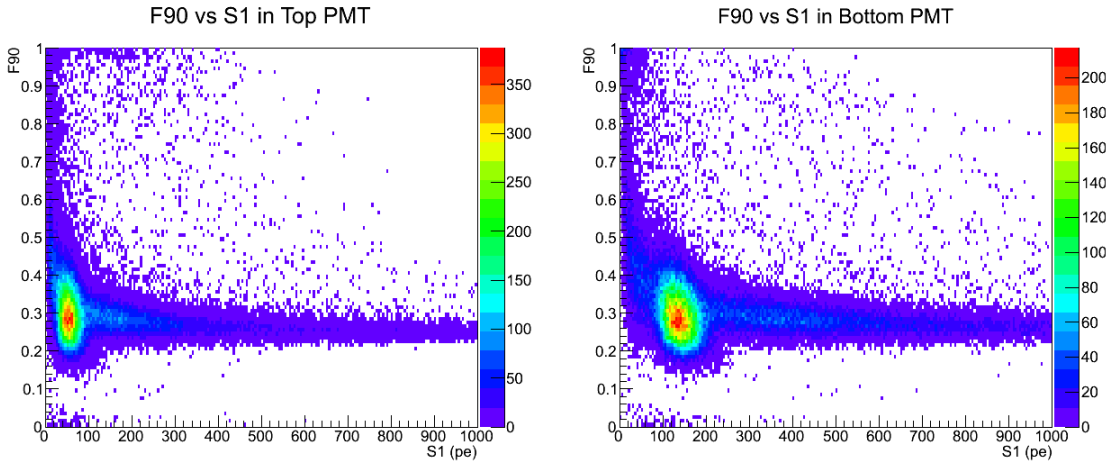

Figure 4.2: 2D Histograms of the two PMT's response to the ^{83m}Kr source. The source deposited a pair of gammas resulting in a total energy deposition of 41.5 keV. The vertical axis of each plot is the pulse shape discrimination parameter F90.

Using the ^{83m}Kr source uniformly present in the liquid argon, a comparison between the average energy of the event (41.5 keV) and the PMT response can be made. The source being used decays via a pair of electromagnetic transitions, so the events will be electron-recoiling events. The measurement has units of photoelectrons per kiloelectron-volt electron equivalent (PE/keVee) to denote that this is a measurement using an electron-recoil source.

Figure 4.2 shows the distribution of events passing all of the cuts except the F90 cut, in order to show the full F90 spectrum. Events were required to have an F90 between 0.2 and 0.4. This cuts off any nuclear recoil events, since we know we are looking for an electron recoil. We cannot cut against high energy cosmic rays, though fitting for the light yield is performed on peak along S1 $\pm$50 pe.

The light yield is sensitive to the strength of the drift field present. A stronger drift field will accelerate free electrons away from their parent, removing the ionized scintillation pathway for the argon excimer. Since it is the recombination and subsequent de-excitation of the argon that causes the scintillation, reducing the number of free electrons available to recombine at the event site. The value reported for the light yield of a TPC is given for a null drift field, where the maximum scintillation response is observed. The peak light yield for each the atmospheric argon and underground argon are given in table4.1

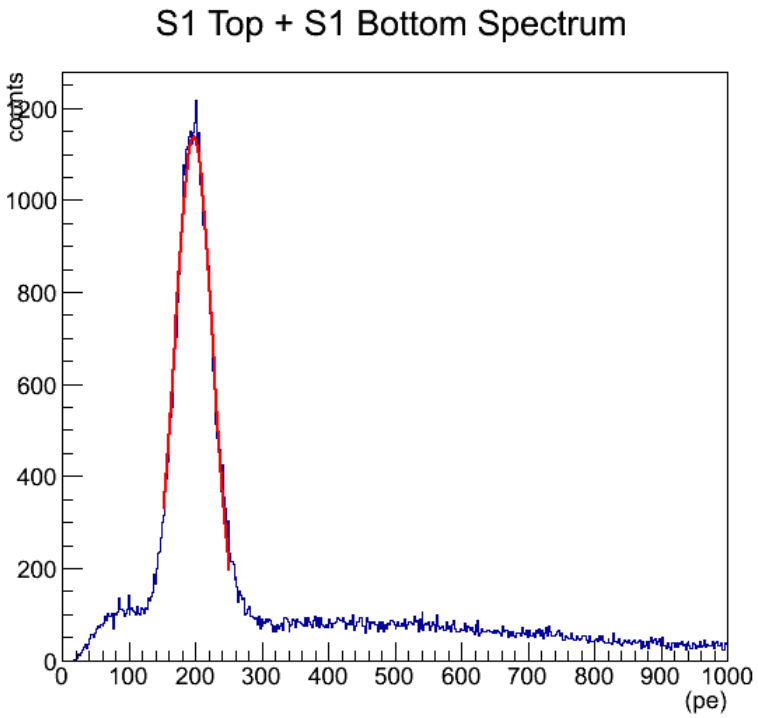

Figure 4.3: The top and bottom tube S1 signal, summed. The red line denotes a gaussian function fit to the peak from the ^{83m}Kr source.

Atmospheric Argon	4.5 ± 0.2 PE/keVee
Underground Argon	4.7 ± 0.2 PE/keVee

Table 4.1: Light Yield measured at the end of each the atmospheric argon runs and the underground argon runs. Data compared is in S1+S2 mode.

The light yield continued to improve throughout the campaign, as the getter continued to improve conditions. Figure4.4 shows the increase of the light yield over the course of the S1 + S2 data collection of the Underground Argon run. The Green line indicates when the recirculation rate was greatly reduced, as described in section 1. Following the collection of S1 + S2 data, the recirculation was increased, and then turned off to take a run, to get the high purity result shown in table 4.1. This end-of-campaign recirculation also served to produce the runs analyzed for the triplet state lifetime.

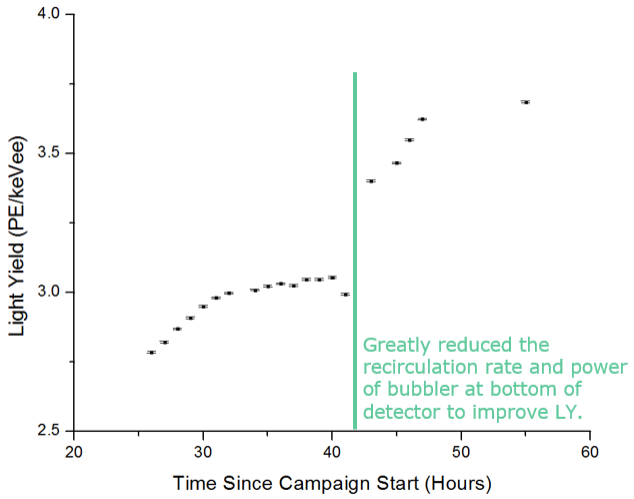

Figure 4.4: Light Yield of S1 + S2 runs, with accompanying statistical errors.

4.4 Triplet State Lifetime

There are two main components to the argon scintillation. A fast component which occurs in the first 150 nanoseconds, and a tailing slow component that occurs over the following 7 microseconds. The fast component is a response from the singlet state de-excitation in argon, the slow component is a response to the triplet state de-excitation. The lifetime of this triplet state is another valid way to measure the purity of the liquid argon. This lifetime has been previously measured.[22] We can compare the lifetime of this triplet state between underground argon and atmospheric argon for events with a given energy range, looking for a similar response.

The lifetime of the slow component can be measured by making an "average waveform," summing the raw waveform of all selected events allows us to see the slow decay of the S1 pulse. Fitting was performed on the waveforms created in the bottom PMTs from 0.7 microseconds to 7 microseconds, following the method performed to validate previous results on this detector. The top PMT was omitted from this study, due to light loss effects reducing the ability of the top PMT to see the full light. While the slow triplet decay begins well before the 1 microsecond fit limit, we are motivated to avoid that region due to a spike near 400 nanoseconds. Previously documented helium contamination in the SCENE detector has led to a small afterpulsing signal in the tube itself. To avoid this hardware effect, the fit is started well after the afterpulse occurs.

Waveforms were fit to the equation

$$y = Ae^{\frac{-t}{\tau}} + B \tag{4.1}$$

where A is an arbitrary amplitude and τ is the lifetime constant of the slow component's decay. This lifetime constant is a detector independent measure of purity and is measured. Lippincott et. al [22] report a lifetime of $1463 \pm 5_{stat} \pm 50_{sys} ns$, while Hitachi et. al [33] reports $1600 \pm 100 ns$.

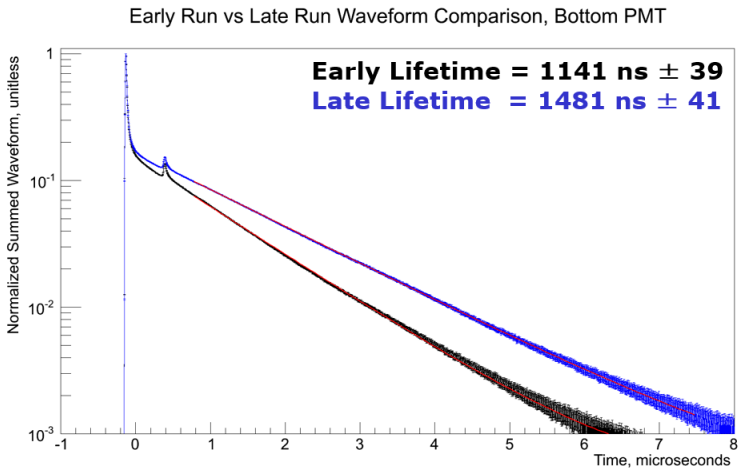

Figure 4.5: Comparison of S1 only runs taken before the S1 + S2 data taking, and after completing the S1 + S2 data collection. The runs were normalized to the maximum of the fast component for comparison's sake.

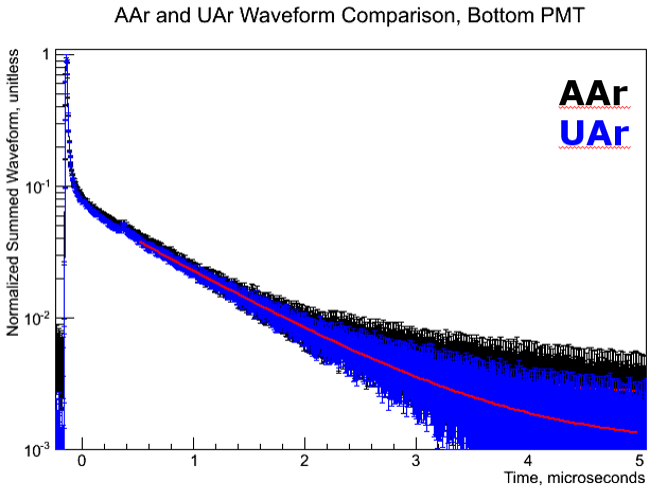

Figure 4.6: Comparison of slow component summed waveforms for Underground argon (blue) and Atmospheric argon (black.) This particular comparison is between two runs in the S1 + S2 mode with a drift field of 50 V/cm. This particular set was chosen due to the similarity of their running conditions. UAr and AAr runs were normalized to the maximum of the fast component for comparison's sake.

Making a direct comparison between the atmospheric and underground argon runs (Fig. 4.6) required abandoning published values and looking at the waveforms qualitatively. The events used were selected from the ^{83m}Kr energy region for similar

runs in AAr and UAr. This region was chosen because it represents the same kind of event, in large enough quantity, to make a comparison between the two. In the case of looking at the summed, time dependent waveform, the 222 ns delay between the two electromagnetic transitions in the ^{83m}Kr affects the observed lifetime, which measures close to 1 μs. The atmospheric argon has a slightly longer lifetime constant in this comparison.

4.5 Drifting Electrons

Two valuable measurements can also be made to the secondary scintillation, which is a product of the ionized electrons drifting across the detector into the argon gas pocket. First, looking to see that electrons can drift from the bottom of the detector all the way to the top. The free electrons have a slow (mm/μs) velocity in the liquid argon dependent on the electric field strength.[34]) We observe the drift time for two electric field strengths, 50 V/cm and 200 V/cm. The drift speed of electrons drifting

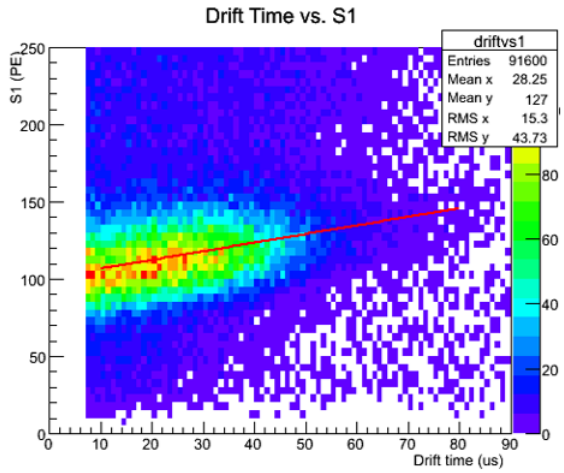

Figure 4.7: Drift time vs S1 for the first data collected in S1 + S2 mode. Drift field was set to 200 V/cm while the argon continued to be purified. Most of the accepted events are in the top half of the detector.

in liquid argon has been characterized[34], allowing for the maximum drift time to be known for a given drift field. This speed is typically in the range of millimeters per microsecond. When the S2 mode data collection began, events with energies relatable to the ^{83m}Kr source were found primarily near the top of the detector. The drift field was held constant at 200 V/cm over the next 12 hours during strong recirculation. Live analysis of the data was not possible, so the heavy recirculation was halted after pausing and observing a uniform distribution along the z-axis of the detector.

Though slightly unfair, comparisons to the Darkside-50 detector can be made. That cryostat is much larger, and reports drift times of $> 300\mu$s at 200V/cm drift

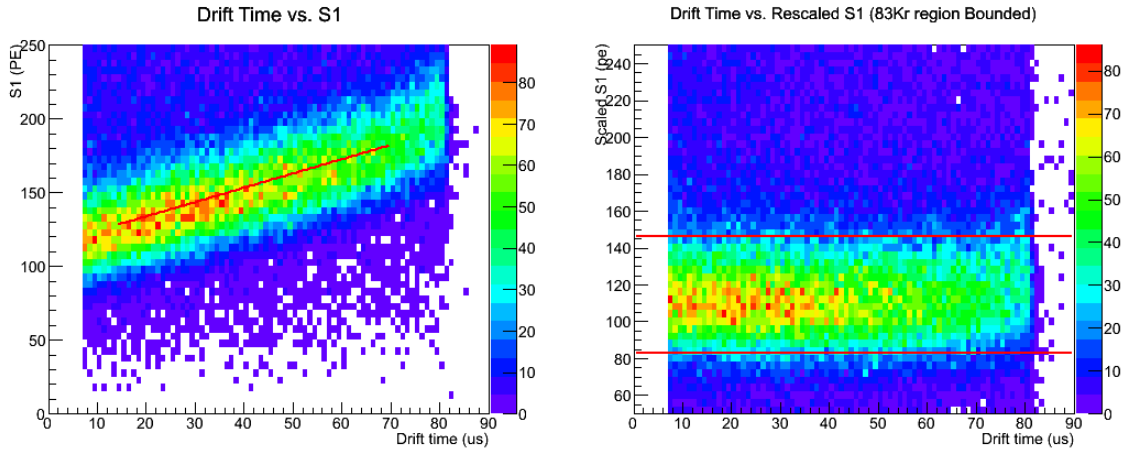

Figure 4.8: Left: Drift vs S1 at the end of the rigorous purification of the UAr. Linear fit made to the slope as a function of drift time. Right: Visualization of the linear correction factor applied to the events, with the ^{83m}Kr mean centered between $\pm 1\sigma$ red bands. This set of events will be used for further analysis. This shift also makes it easier to see that the events are distributed evenly throughout the height of the detector.

field. Runs with a 50 V/cm drift field were also collected to observe the ability of the detector to drift for longer than 100 μs. Even by the end of the campaign, the distribution of events was not uniform along the drift axis of the detector, like seen in the 200 V/cm drift field data. This is an observed similarly in both the atmospheric argon and underground argon data from this campaign, and qualitatively similar to the data reported in ref.[20].

A further interesting feature is seen when plotting drift time against S1. The average energy trends towards higher PE count as we get towards the bottom of the detector. The bottom PMT's response is typically much stronger due to the liquid-gas reflection, as well as shadow from the grid. The PMT used at the top of the detector has a much smaller signal likely related to degradation of the PMT itself. This feature can be accounted for by fitting a linear function to the means of each bin in drift time.

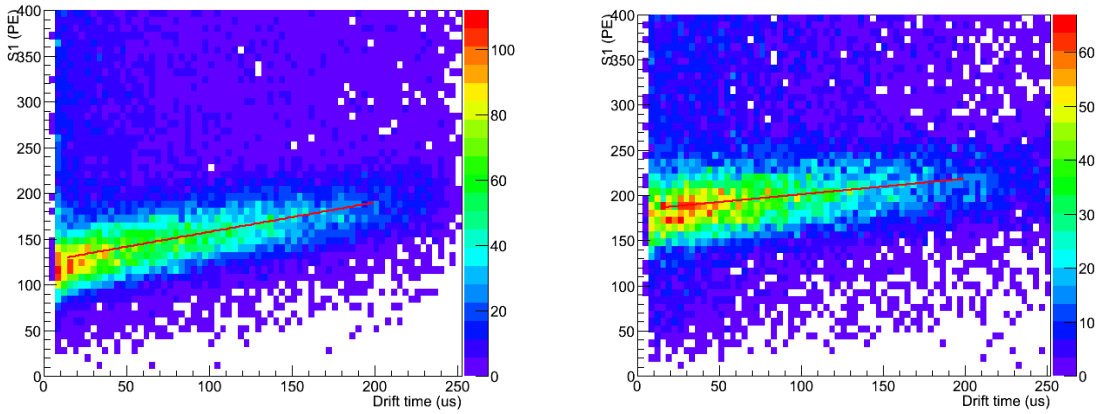

Figure 4.9: Left: Achieved drift vs S1 in atmospheric argon for 50V/cm drift field. Right: The same, for underground argon. Both exhibit the ability to drift electrons from the limit of 238 microseconds[34], though neither shows the uniform distribution of events that 200 V/cm runs do, showing the limit of this purification.

While the drift time data presented gives a largely qualitative picture, it shows that we are happy. At a typical running drift field strength of 200 V/cm we are able to drift electrons throughout the entire detector at a largely uniform rate. When the applied field is lowered, we see results comparable between the atmospheric argon run and underground argon run of this campaign, which agrees with ref. [20].

4.6 Electron Drift Lifetime

The number of electrons able to reach the gas pocket is related to the position of the event along the drifting axis and the event energy. The size of the S2 signal will be proportional to the number of electrons that reach the gas pocket at the top of the detector. By picking events in a specific energy region, and of a specific recoil type, we can relate the strength of the S2 signal to the drift time to find a lifetime of the electrons, often referred to as the electron drift lifetime. To calculate this "lifetime

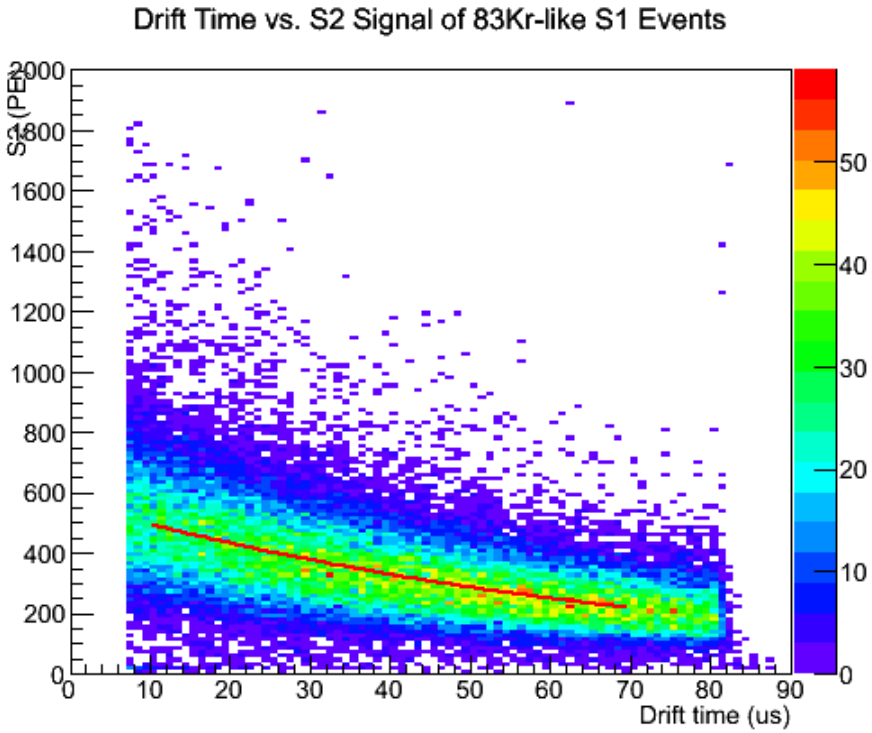

Figure 4.10: Drift Time vs S2 plotted for events which have been identified as ^{83m}Kr events. The red line denotes an exponential decay fit to the means of S2 as a function of drift time. This plot is of data taken with a drift field of 200V/cm.

constant", histograms of the total S2 for an event were created in 3 microsecond sections of drift time. A Gaussian was fit to the peak in S2. The means of these fits are plotted vs their respective drift times, and an exponential decay function was fit

to the means, weighted by the errors associated with the means. In 200 V/cm data, the lifetime was fit from 10 μs to 70 μs to avoid edge effects.

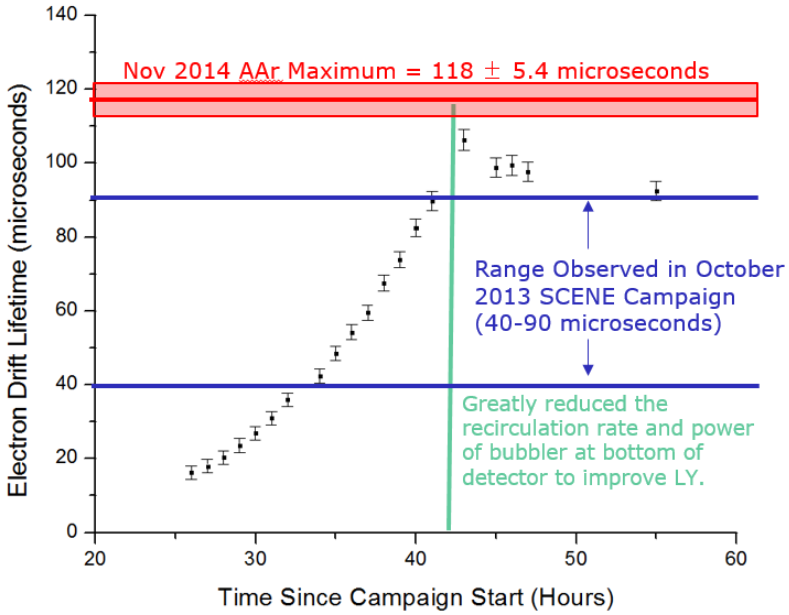

Figure 4.11: Comparison between Atmospheric (left) argon and Underground (right) argon drift times vs S1 for the last 50 V/cm run in each test. The yellow line denotes the drift time limit at 50 V/cm drift field.

The electron drift lifetime observed in the underground argon campaign improves with time while recirculating heavily. When the recirculation rate was reduced, the electron drift lifetime began to decrease, slowly. As seen in Figure 4.11, the observed electron drift lifetime started well below the value reported by the SCENE collaboration in ref.[20], and once the recirculation was reduced, maintained a lifetime longer than observed previously in SCENE.

Unfortunately, the underground argon run did not manage to reach the 118 ± 5.4 μs maximum lifetime observed in the atmospheric argon run of this campaign. This is likely due to the length of the atmospheric argon purification: The atmospheric run allowed the argon to purify over the course of 3 weeks, whereas the underground argon run lasted for 4 days. The underground argon run was kept short the reduce

the likelihood of an emergency power failure, and to meet shipping deadlines for the underground argon.

Still, when combined with the other results, the question of the viability of this argon to be used in DarkSide-50 was clearly true. Light yield values for atmospheric argon and underground argon are consistent within error to each other. The gas was purified until the argon produced a lifetime consistant with published work. The electrons are able to drift from all points in the detector in a common field configuration, and are able to drift in very low drift fields successfully. Finally, the electron drift lifetime validates the ability for over half of the electrons drifting from the bottom to make it to the top without capture.

CHAPTER 5

CLOSING COMMENTS

The argon from the Cortez, CO based CO2 well was purified at Fermilab in Batavia, IL. The gas was then condensed inside a small, dual phase TPC to observe it's ability to scintillate and drift electrons. The chief concern was trace levels of impurities unaccounted for that would be able to pass the zirconium getting planned as the final step for the whole supply of argon at the time of insertion into the DarkSide-50 detector. Both the ability to scintillate and drift electrons were confirmed.

This research came to conclusion December 15th, 2014. With the collaboration interested in switching from atmospheric to underground argon as soon as possible, this work made it clear that we were safe to ship the argon to Italy as a finished product. The argon left the Proton Assembly building on December 17th, and filling of DarkSide-50 began in April.

If this campaign had not been successful, it is likely that the argon would not have been shipped by the end of the year, a collaboration goal. The detector site at LNGS is not ideal for R&D style purification. Based on the failure, further analysis would have been conducted and additional purification would have taken place at the PAB. Thankfully, this was not necessary.

By the time of this thesis' publication, the first results from the Underground Argon run of DarkSide-50 have begun to trickle out. Unlike SCENE in this campaign, DarkSide-50 is acutely sensitive to the ^{39}Ar content present in the underground argon. While previous works indicated an upper limit of 150 times less ^{39}Ar in our product, the collaboration is now confidently reporting[35] a reduction factor of at least 300.

Figure 5.1: Dr. Henning Back and Dr. Stephen Pordes, watching the packed shipment of Underground Argon make its first step towards the detector in Italy. Henning and Stephen looked like proud parents watching their child get on the school bus for the first time. Kelly Hardin, part of the staff responsible of building the purification system at FNAL, did the honors.

BIBLIOGRAPHY

[1] F. Zwicky, "Die Rotverschiebung von extragalaktischen Nebeln," *Helvetica Physica Acta*, vol. 6, pp. 110–127, 1933.

[2] V. C. Rubin, D. Burstein, W. K. Ford, Jr., and N. Thonnard, "Rotation velocities of 16 SA galaxies and a comparison of Sa, Sb, and SC rotation properties," *apj*, vol. 289, pp. 81–98, Feb. 1985.

[3] A.-M. Weijmans, D. Krajnovic, G. van de Ven, T. A. Oosterloo, R. Morganti, and P. T. de Zeeuw, "The shape of the dark matter halo in the early-type galaxy NGC 2974," *Mon. Not. Roy. Astron. Soc.*, vol. 383, p. 1343, 2008.

[4] M. Aartsen *et al.*, "IceCube Search for Dark Matter Annihilation in nearby Galaxies and Galaxy Clusters," *Phys.Rev.*, vol. D88, p. 122001, 2013.

[5] P. Agnes, T. Alexander, A. Alton, K. Arisaka, H. Back, *et al.*, "First Results from the DarkSide-50 Dark Matter Experiment at Laboratori Nazionali del Gran Sasso," *Phys.Lett.*, vol. B743, pp. 456–466, 2015.

[6] LIDINE2013, "http://iopscience.iop.org/1748-0221/focus/extra.proc28."

[7] B. Baller, N. Buchanan, F. Cavanna, H. Chen, E. Church, *et al.*, "Liquid Argon Time Projection Chamber Research and Development in the United States," *JINST*, vol. 9, p. T05005, 2014.

[8] B. Jones, C. Chiu, J. Conrad, C. Ignarra, T. Katori, *et al.*, "A Measurement of the Absorption of Liquid Argon Scintillation Light by Dissolved Nitrogen at the Part-Per-Million Level," *JINST*, vol. 8, p. P07011, 2013.

[9] B. Jones, T. Alexander, H. Back, G. Collin, J. Conrad, *et al.*, "The Effects of Dissolved Methane upon Liquid Argon Scintillation Light," *JINST*, vol. 8, p. P12015, 2013.

[10] D. E. Grosjean, R. A. Vidal, R. A. Baragiola, and W. L. Brown, "Absolute luminescence efficiency of ion-bombarded solid argon," *Phys. Rev. B*, vol. 56, pp. 6975–6981, Sep 1997.

[11] T. Alexander, D. Alton, K. Arisaka, H. Back, P. Beltrame, *et al.*, "Light yield in DarkSide-10: A prototype two-phase argon TPC for dark matter searches," *Astroparticle Physics*, vol. 49, pp. 44–51, Sept. 2013.

[12] P. A. Amaudruz *et al.*, "DEAP-3600 Dark Matter Search," in *International Conference on High Energy Physics 2014 (ICHEP 2014) Valencia, Spain, July 2-9, 2014*, 2014.

[13] J. Xu, F. Calaprice, C. Galbiati, A. Goretti, G. Guray, *et al.*, "A Study of the Residual 39Ar Content in Argon from Underground Sources," *ArXiv e-prints*, Apr. 2012.

[14] J. Xu, *Study of Argon from Underground Sources for Firect Dark Matter Detection*. PhD thesis, Princeton University, Princeton, NJ, 9 2013.

[15] H. O. Back, F. Calaprice, C. Condon, E. de Haas, R. Ford, *et al.*, "First Large Scale Production of Low Radioactivity Argon From Underground Sources," *ArXiv e-prints*, Apr. 2012.

[16] H. O. Back, T. Alexander, A. Alton, C. Condon, E. de Haas, *et al.*, "First Commissioning of a Cryogenic Distillation Column for Low Radioactivity Underground Argon," *ArXiv e-prints*, Apr. 2012.

[17] T. Alexander, H. O. Back, H. Cao, A. G. Cocco, F. DeJongh, *et al.*, "Observation of the dependence on drift field of scintillation from nuclear recoils in liquid argon," *Phys.Rev.*, vol. D88, no. 9, p. 092006, 2013.

[18] H. Cao, T. Alexander, A. Aprahamian, R. Avetisyan, H. O. Back, *et al.*, "Measurement of scintillation and ionization yield and scintillation pulse shape from nuclear recoils in liquid argon," *Phys. Rev. D*, vol. 91, p. 092007, May 2015.

[19] Saes Pure Gas, "http://www.saespuregas.com/products/gas-purifier/ps4-mt315.html."

[20] H. Cao, *A Study of Nuclear Recoils in Liquid Argon Time Projection Chamber for the Direct Detection of WIMP Dark Matter*. PhD thesis, Princeton University, Princeton, NJ, 11 2014.

[21] Cryomech, "http://www.cryomech.com/products/cryorefrigerators/pulse-tube/pt60/.."

[22] W. Lippincott, K. Coakley, D. Gastler, A. Hime, E. Kearns, *et al.*, "Scintillation time dependence and pulse shape discrimination in liquid argon," *Phys.Rev.*, vol. C78, p. 035801, 2008.

[23] I. Vikuiti enhanced specular reflector by 3M, "www.3m.com."

[24] Sigma Aldrich, "http://www.sigmaaldrich.com/catalog/product/aldrich/185213."

[25] R. Francini, R. Montereali, E. Nichelatti, M. Vincenti, N. Canci, *et al.*, "VUV-Vis optical characterization of Tetraphenyl-butadiene films on glass and specular reflector substrates from room to liquid Argon temperature," 2013.

[26] Hamamatsu Photonics., "www.hamamatsu.com."

[27] V1720B Digitizers by CAEN S.p.A, "http://caen.it."

[28] B. Loer, "Daqman on Github. http://github.com/bloer/daqman."

[29] Lake Shore Cryotronics, Inc. Model 336, "http://www.lakeshore.com/products/cryogenic-temperature-controllers/model-336/."

[30] National Instruments, "http://www.ni.com/labview/."

[31] USB-1208LS Multifunction USB Data Acquisition Device from Measurement Computing Corporation., "http://www.mccdaq.com/usb-data-acquisition/usb-1208ls.aspx."

[32] Smartec, "http://www.smartec-sensors.com/en/products/uti-interface-en.html, universal transducer interface."

[33] A. Hitachi, T. Takahashi, N. Funayama, K. Masuda, J. Kikuchi, and T. Doke, "Effect of ionization density on the time dependence of luminescence from liquid argon and xenon. Phys. Rev. B 27, 5279 (1983).,"

[34] P. Cennini *et al.*, "Performance of a three-ton liquid argon time projection chamber," *Nuclear Instruments and Methods in Physics Research Section A: Accelerators, Spectrometers, Detectors and Associated Equipment*, vol. 345, no. 2, pp. 230 – 243, 1994.

[35] A. Fan, "Status and results of darkside-50," *DPF 2015*, Aug 2015.